

Keywords

ZnO,
Ni-doped ZnO,
Raman Spectroscopy

Received: March 12, 2017

Accepted: March 30, 2017

Published: June 7, 2017

Raman Spectroscopic Studies of Nickel- Oxide Doped ZnO Nanoparticles

Mohamed A. Elbagermi^{1, *}, Adel I. Alajtal¹, Hoell G. M. Edwards²,
Aditya Sharma³, keshav deo Verma³

¹Department of Chemistry, Faculty of Science, University of Misurata, Misurata, Libya

²Raman Spectroscopy Group, University Analytical Centre, Division of Chemical and Forensic Sciences, University of Bradford, West Yorkshire, UK

³Material Science Research Laboratory, Department of Physics, S. V. College, Aligarh, (U.P.), India

Email address

M.elbagermi@yahoo.co.uk (M. A. Elbagermi)

*Corresponding author

Citation

Mohamed A. Elbagermi, Adel I. Alajtal, Hoell G. M. Edwards, Aditya Sharma, keshav deo Verma. Raman Spectroscopic Studies of Nickel- Oxide Doped ZnO Nanoparticles. *Journal of Materials Sciences and Applications*. Vol. 3, No. 2, 2017, pp. 23-27.

Abstract

Zn_{1-x}Ni_xO (x = 1mol%, 3mol% and 5mol%) powders were prepared by a simple co-precipitation method and analysed using X-ray diffraction (XRD) and Transmission Electron Microscopy (TEM). The XRD measurements revealed the formation of single phase Ni- doped ZnO up to Ni concentrations of x = 0.03. The Zn_{0.95}Ni_{0.05}O sample shows the formation of a secondary phase of NiO, which indicates the solubility limit of Ni in the ZnO matrix. The TEM micrograph shows the estimated grain size of doped & undoped ZnO to be approximately 20nm. Raman spectra of ZnO nanoparticles (ZnO-NPs), as well as the transition-metal-doped (5% Nickel) ZnO nanoparticles with the average size of 20 nm have been measured. A characteristic Raman peak at 434 cm⁻¹ is observed in the ZnO-NPs, whereas the doped Zn_{1-x}Ni_xO specimens (x= 1mol%, 3mol% and 5mol%) showed characteristic peaks shifted in wavenumber at 434, 430, and 425 cm⁻¹, respectively. These peaks can be related to the formation of NiO species in the doped ZnO-NPs.

1. Introduction

Wurtzite-type ZnO is an interesting material for optoelectronic devices. Recently, nanostructures made of ZnO have attracted significant attention owing to their proposed applications in low-voltage and short-wavelength electro-optical devices, transparent ultraviolet protection films and even spintronic devices [1- 3]. In this sense, diluted magnetic semiconductors (DMS) have attracted much scientific interest in the last few decades owing to their unique properties, with possible technological applications utilizing both semiconductor physics and ferromagnetism so called 'spintronics'. Transition-metal -doped ZnO systems are highly promising DMS candidates for applications requiring ferromagnetic behavior near room temperature [4]. We have here doped ZnO with Ni in order to examine the influence of Ni dopant on the free charge-carrier properties of the Zn-O host matrix.

Raman spectroscopy has been a nondestructive characterization method of choice for many recent studies of the vibrational properties of ZnO nanostructures [5, 6]. Moreover,

this technique is very versatile for the study of dopant incorporation, particularly when impurity-induced modes can be attributed to the individual constituents [7-9].

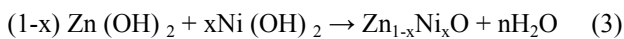
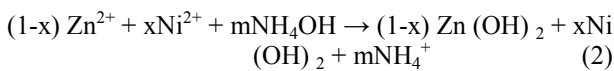
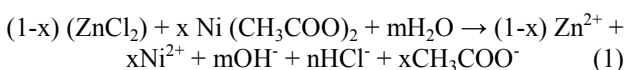
ZnO is a semiconductor with a hexagonal wurtzite crystal structure belonging to the space group C_{6v}^4 with two formula units per primitive cell, where all atoms occupy C_{3v} sites. The Raman activity of the zone-center optical phonons predicted by the group theory is $A_1+2E_2+E_1$. The phonons of A_1 and E_1 symmetry are polar phonons and exhibit different wavenumbers for the transverse-optical (TO) and longitudinal-optical (LO) phonons. Nonpolar phonon modes with symmetry E_2 have two discrete wavenumbers: E_2 (high) is associated with oxygen atoms and E_2 (low) is associated with the Zn sub lattice. All of the predicted phonon modes have been reported in the Raman scattering spectra of bulk ZnO [10-14].

In this work, we report for the first time the Raman spectroscopic study of ZnO-NPs and Ni-doped ZnO-NPs. The objective of this study was to review the vibrational modes of ZnO-NPs and to obtain information regarding the existence of additional modes which could be attributed specifically to dopant Ni atoms.

2. Experimentation

2.1. Sample Preparation

Pure and Ni- doped zinc oxide nanoparticles were prepared using a co-precipitation method. All the reagents were of analytical grade and were used without further purification. $ZnCl_2 \cdot 5H_2O$ and $Ni(CH_3COO)_2 \cdot 5H_2O$ were dissolved in de-ionized water with magnetic stirring until they form clear solutions. Ammonium hydroxide (0.1M) solution was then added drop-wise into the clear solution of zinc chloride and nickel acetate with constant magnetic stirring and then ageing for 30 minutes. The pH value of the solution was maintained at a pH of 7 during the synthesis of all samples. The resultant white precipitates were washed several times with de-ionized water to remove Cl^- ions and other ionic impurities. The precipitates were dried in air at 40 °C and the light yellow colored powders were collected. The nickel doping ratio x was the molar ratio of Ni to Ni+Zn. This procedure was followed for all compositions of the nickel- doped zinc oxide samples. From the nature of synthesis and experimental observation, the formation of the $Zn_{1-x}Ni_xO$ nanoparticles in the colloidal medium would probably occur via the following reaction scheme;



In the reaction solution, zinc chloride, nickel acetate and ammonium hydroxide undergo ionic dissociation to form

Zn^{2+} , Ni^{2+} , OH^- and NH_4^+ ions. The intermediate hydroxides of Zn $(OH)_2$ and Ni $(OH)_2$ are expected to combine and form $Zn_{1-x}Ni_xO$ granules in the colloidal medium. Radovanovic *et al.* [12] have reported the formation of $Zn_{1-x}Ni_xO$ nanocrystalline powders using a wet chemical method (core/shell procedure), but they could not achieve a reproducible size/shape controlled growth of nanoparticles. In previous report [15, 16], of the synthesis of $Sn_{1-x}Co_xO_2$ nanoparticles, we have achieved almost mono-disperse nanoparticles of spherical shape, without adding any surfactant and/or capping agent using the procedure outlined above. The similar synthesis procedure, with a pH =7 at 40°C, employed in the present work, may therefore be suitable for us to prepare, $x = 0.00$ to 0.05 , nickel doped ZnO nanoparticles of a single phase nature.

2.2. Instrumentation

Raman spectra were obtained using an Almega XR dispersive Raman spectrometer. An Olympus microscope (B x 51) and an Olympus x 50 objective (NA=0.80) were used both for focusing the laser on the sample, to a spot size ~ 1 μm diameter, and for collecting the scattered light in a 180° backscattering configuration. The scattered light was detected by a charge coupled device (CCD) detector, thermoelectrically cooled to -50°C. The spectrometer used a grating (675 lines/ mm) to resolve the scattered radiation and a notch filter to block the Rayleigh light. The pinhole of the monochromator was set at 25 μm . The Raman spectra were accumulated over 80 s with a resolution of ~ 4 cm^{-1} . The excitation source was the 532 nm radiation from an Nd:YVO₄ laser (frequency- doubled).

3. Results and Discussion

3.1. XRD and TEM Analysis

Figure 1 is the XRD pattern of the $Zn_{1-x}Ni_xO$ ($x=0, 0.01, 0.03, 0.05$) samples. The XRD patterns show that there is no second-phase peak and the doping powder X-ray diffraction patterns of undoped ZnO and Ni-doped ZnO are shown in figure 1. The characteristic peaks with high intensities corresponding to the planes (100), (002), (101) and lower intensities at (102), (110), (103), (200), (112), and (201) indicate the annealed product is a high purity hexagonal ZnO wurtzite structure. It's evident from the XRD data that there are no additional peaks due to nickel metal, other oxides or any zinc nickel phase, indicating that the synthesized samples are all single phase. Hence, we can infer that the Ni ion has substituted in the Zn sites without changing the wurtzite structure.

The peaks of the diffraction patterns of the doped samples appear to be narrow compared with the undoped ZnO. This shows that only a small variation in the lattice parameters occurs as the Ni concentration in the sample increases. The length of both the a and c axes increases monotonically with the increasing Ni doping in ZnO. The expansion of the lattice

constants and the slight shift of XRD peaks with the different concentration of Ni doped ZnO specimens indicated that nickel has effectively become substituted into the ZnO structure. The average crystal size (D) was estimated using the Scherrer relation ($D=0.9\lambda/\beta \cos\theta$, where β is the FWHM

of the XRD peaks and λ is the wavelength of incident x-rays). The crystal size of the undoped ZnO on subsequent doping of Ni shows an increasing tendency with concentration of the dopant.

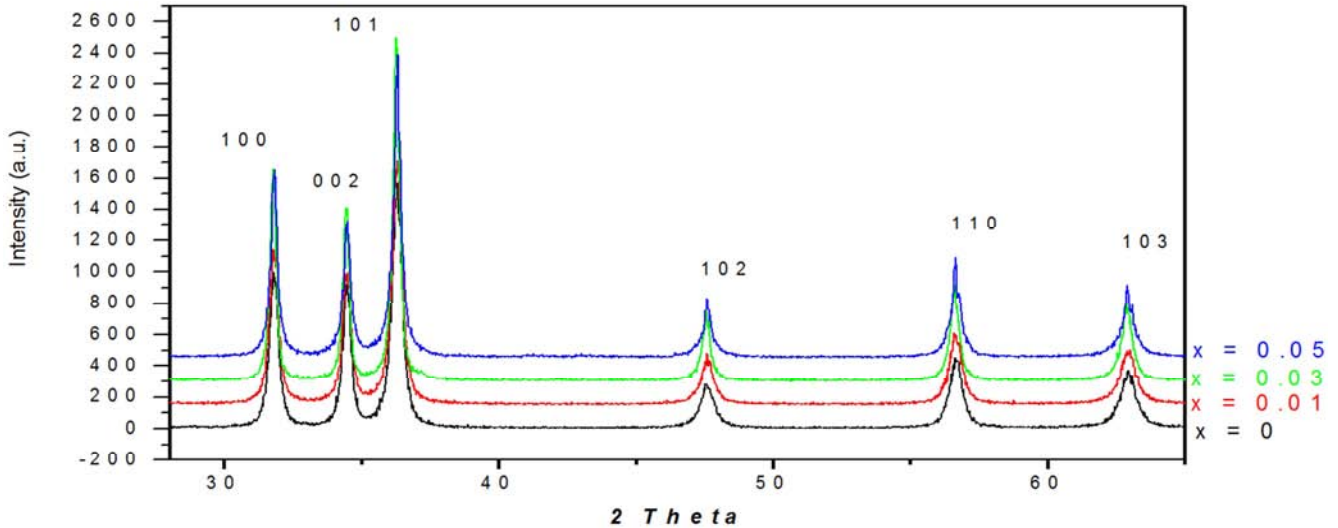


Figure 1. The X-Ray Diffraction (XRD) pattern for the $Zn_{1-x}Ni_xO$ with, ($x=0.0, 0.01, 0.03, 0.05$) samples.

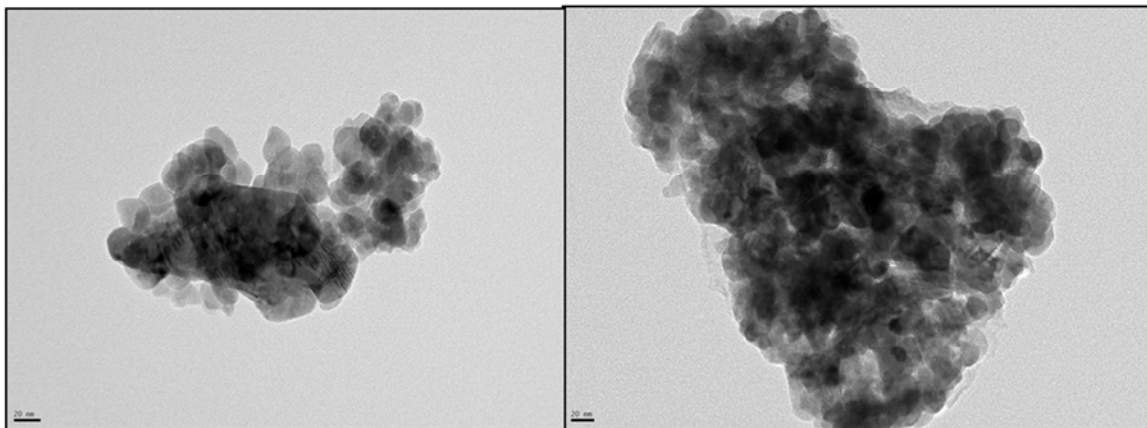


Figure 2(a). The Transmission electron microscopy (TEM) for the Pure ZnO & 1% Ni-doped ZnO.

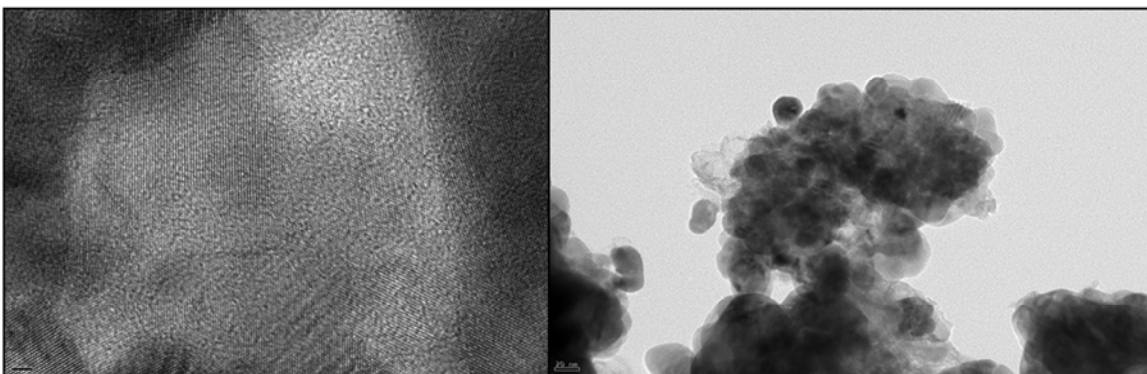


Figure 2(b). The Transmission electron microscopy (TEM) for the 3%Ni-doped ZnO & 5%Ni-doped ZnO.

These results are in good agreement with those obtained from TEM measurements. A minor increase in lattice parameters ('a' & 'c') and unit cell volume was observed with increasing nickel concentration indicates the substitution

of nickel in the zinc oxide lattice; it is expected that the substitution of the transition metal ions may cause dilation in the wurtzite structure. Figure 2 shows the TEM image of the Pure and Ni-doped ZnO nanoparticles. The TEM image

indicates that nanoparticles are formed with only a spherical shape. However, a significant aggregation of the nanoparticles is also observed. This aggregation makes it difficult to determine the crystal size accurately but we estimate the size from individual spherical nanocrystal measurements to be ~ 20 nm.

3.2. Raman Spectroscopy of Pure and Ni-Doped ZnO-NPs Analysis

Figure 3 shows the Raman spectra of ZnO-NPs and Ni-doped ZnO-NPs. The Raman spectrum of the nanoparticles has been scaled up by a factor of two relative to that of the pure zinc oxide nanoparticles. In the pure ZnO spectrum, the peak at 329 cm^{-1} is attributed to the second-order Raman processes, the peak at 434 cm^{-1} corresponds to E_2 (high) and the peak at 580 cm^{-1} is positioned between the A_1 (LO) and E_1 (LO) modes. In these spectra, no shift of the Raman peaks at 329 cm^{-1} and 434 cm^{-1} is observed for 1% Ni-doped ZnO. Moreover, this figure also shows the Raman spectra of 3%

and 5% Ni-doped ZnO, with characteristic bands corresponding to $[E_2$ (high)] at 430 cm^{-1} and 425 cm^{-1} , respectively, indicating a decrease in characteristic peak wavenumber with the increase of Ni doping. These peaks can be related to the formation of NiO species in the doped ZnO-NPs.

This figure also shows the A_1 (TO) peaks for Pure & $Zn_{1-x}Ni_xO$ samples at 329 cm^{-1} (pure), 329 cm^{-1} (1%), 326 cm^{-1} (3%) and 318 cm^{-1} (5%), respectively, in decreasing order and also exhibits the E_1 (LO) peaks for pure & $Zn_{1-x}Ni_xO$ at 580 cm^{-1} (Pure), 574 cm^{-1} (1%), 571 cm^{-1} (3%), and 562 cm^{-1} (5%), respectively, also in decreasing order. It can therefore be stated that with an increase in Ni-doping in a ZnO matrix then the observed wavenumber of the peak is decreased. In this study, we see a similarity between the doped samples and the corresponding standard spectra and that the incorporation of Ni ions into the ZnO matrix is therefore related to intrinsic host lattice defects which then become spectroscopically vibrationally active.

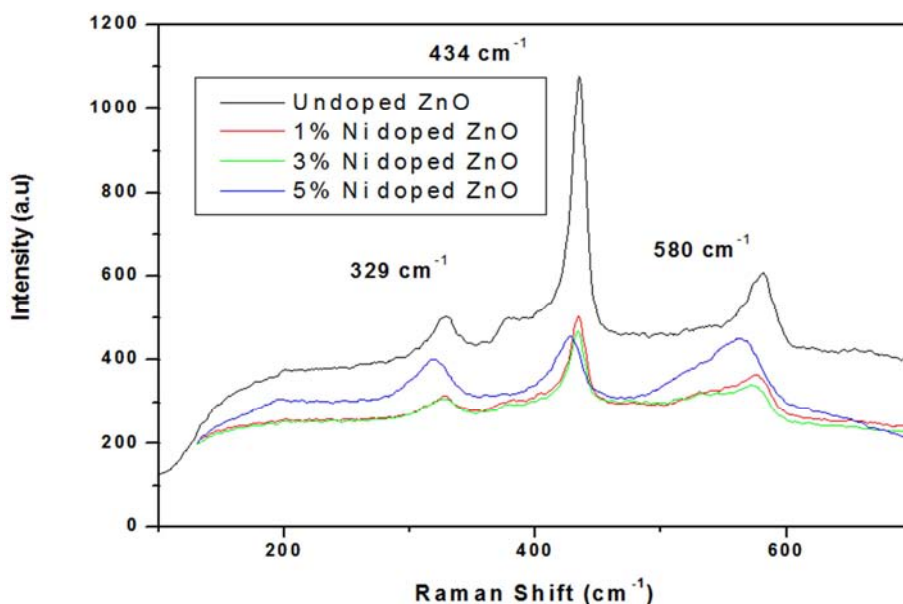


Figure 3. Raman Spectra of Pure and Ni-doped ZnO nanoparticles.

4. Conclusions

ZnO powders containing the transition metal Ni synthesized by a simple hydrothermal process correspond to a hexagonal structure similar to that of undoped ZnO. The XRD measurements suggest that Ni atoms substitute in Zn sites in the crystals without changing the wurtzite structure, but with the lattice parameters varying slightly with the extent of doping. The average grain sizes for different samples obtained from XRD measurement are in good agreement with those obtained from TEM measurements. No secondary phases were observed for the simple synthesis process adopted in the present work for the doped ZnO samples up to 5mol% of Ni doping.

The Raman spectra of ZnO-NPs did not show any new modes at different laser powers and, furthermore, we did not

observe a shift of the Raman peak (434 cm^{-1}), in the 1% Ni-doped ZnO-NPs. It was observed that the additional modes appear only in the spectra of ZnO with Ni dopant concentrations above 3%, such as the peak at 430 cm^{-1} for the 3% Ni-doped and 425 cm^{-1} for the 5% Ni-doped ZnO nanoparticles, which can be related to the magnetic ions found in the studied matrix. These modes seem to be related to the individual dopant and may be used as an analytical indicator for their incorporation.

References

- [1] R Y Sato-Berru, A Vazquez-Olmos, A L Fernandez-Osorio and S Stores-Martinez, (2007): J. Raman Spectrosc. 38: 1073-1076.
- [2] Y Chen, D M Bagnall, K Park, K Hiraga, Z Zhu, T Yao, (1998): J. Appl. Phys. 84: 3912.

- [3] J Nemeth, G Rodriguez-Gattorno, A Vazquez-Olmos, D Diaz, I Dekany, (2004): *Langmuir*. 20: 2855.
- [4] S J Pearton, C R Abernathy, M E Overberg, G T Thaler, D Norton, N Theodoropoulou, A F Hebard, Y D Park, F Ren, J Kim, L A Boatner, (2003): *J. Appl. Phys.* 93: 1.
- [5] K A Alim, V A Fonoberov, M Shamsa, A A Balandin, (2005): *J. Appl. Phys.* 97: 124313.
- [6] X T Zhang, Y C Liu, Z Z Zhi, J Y Zhang, Y M Lu, D Z Shen, W Xu, G Z Zhong, X W Fan, K G Kong, (2001): *J. Appl. Phys.* 34: 3430.
- [7] C Bundeshmann, N Ashkenov, M Schubert, D Spemann, T Butz, E M Kaidashev, M Lorenz, M Grundmann, (2003): *Appl. Phys. Lett.* 83: 1974.
- [8] Y B Zhang, S Li, T T Tan, H S Park, (2006): *Solid State Commun.* 137: 142.
- [9] W Gebicki, K Osuch, C Jastrzebski, Z Golacki, M Godlewski, (2005): *Superlattices Microstruct.* 38: 428.
- [10] N Ashkenov, B N Mbenkum, C Bundesmann, V Riede, M Lorenz, D Spemann, E M Kaidashev, A Kasic, M Schubert, M Grundmann, (2003): *J. Appl. Phys.* 93: 126.
- [11] J F Scott, (1970): *Phys. Rev. B.* 2: 1209.
- [12] M S H Choudhury, N. Kishi, and T. Soga, (2016): *J. Alloys Compd.* 656: 476-480.
- [13] B Venugopal, B. Nandan, A. Ayyachamy, V. Balaji, S. Amirthapandian, B. K. Panigrahi, and T. Paramasivam, (2014): *RSC Adv.* 4, 6141 – 35743.
- [14] P V Radovanovic and D R Gamelin, (2003): *Phys. Rev. Lett.* 91: 157202.
- [15] A Sharma, A P Singh, P Thakur, N B Brookes, S Kumar, C G Lee, R J Choudhary, K D Verma, and R Kumar, (2010): *J. Appl. Phys.* 107: 093918.
- [16] A Sharma, D. Prakash, and K. D. Verma, (2007): *J. Opto. Adv. Mater.: Rap. Comm.* 1: 683.